Accurate Description of Antibiotics Translocation through Membrane Pores

Enhanced Sampling Methods for Accurate Free Energy Estimates of Antibiotic Permeation Process through Porins

***A. Acharya, P. Behera, U. Kleinekathöfer**, School of Science, Constructor University, Bremen*

In Short

- Antibiotics enter into bacterial cells via outer-membrane channels called porins.
- A precise and quantitative description of the permeation process through porins is a crucial for understanding the dynamics of pore and antibiotic.
- A precise and quantitative characterization of the translocation process through porins is a necessity to understand how different antibiotics permeate.
- The present work has improved the use of temperature-accelerated sliced sampling (TASS) by including MCPS, which eases the setup of the initial system and improves sampling by providing flexibility in generating various configurations. This simplifies and allows users to explore and understand the permeation process of numerous antibiotics and pore dynamics in challenging systems.
- The role of pore electrostatics contributing to the electo-osmotic flow was explored.
- Clinically relevant porins will be explored with various antibiotics.

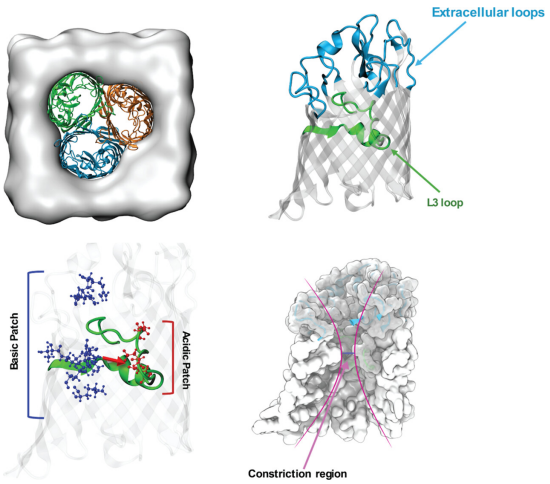

Figure 1: Structure of a typical porin. *The upper panels show OmpK35, which is a trimeric porin embedded in the outer membrane. The loops in blue are the extracellular loop, and the one in green represents the L3 loop. The lower panel shows acid and basic residues contributing to the potential in the porin. The constriction region forms an hourglass structure which acts as a size-exclusion filter. Reproduced with permission from [7]. Copyright 2024 American Chemical Society.*

The outer membrane of Gram-negative bacteria acts as a formidable barrier for extracellular compounds. Vital compounds like nutrients, ions and other solutes are transported using a set of membrane proteins embedded in this outer membrane. These membrane protein transports can be specific transport or passive transport. Porins are a set of outer-membrane proteins that allow passive transport of various solutes including antibiotics [1].

Porins consist of a β-barrel formed by antiparallel β-strands connected by loop regions, creating a water-filled pore with a narrow constriction region (CR). The constriction region (CR) functions as a size-exclusion filter, restricting the passage of solutes with molecular weights up to approximately 600 Da. Numerous experimental and computational studies have elucidated how factors such as solute charge, mass, polarity, pore diameter, and stabilizing interactions within the CR influence permeation rates through these channels [2]. Recent studies emphasize that the presence of an ionizable amine group on the antibiotic scaffold enhances permeation efficiency [3].

Enhanced sampling methods address sampling issues in complex processes such as antibiotic transport. These methods apply additional bias potentials to carry the system out of lower energy states and into higher energy states, where sampling issues exist. Temperature-accelerated sliced sampling has proven efficient for the particular problem of antibiotic transport in the OmpF porin. This method has also helped unravel the mechanism of loop dynamics in the antibiotic permeation process. Our studies have emphasized the internal hydrogen network that stabilizes the L3 loops in various clinically relevant OmpF orthologs in *E. cloacae* and *K. pneumoniae*, which underscores the significant role of loop dynamics in permeation. In the current project, implementing Monte Carlo Pathway Search (MCPS) into TASS has made setting up challenging systems easier and allowed us to address some sampling issues. This involves an independent generation of initial structures of antibiotics inside the pore without affecting the pores initial confirmation unlike steered molecular dynamics.

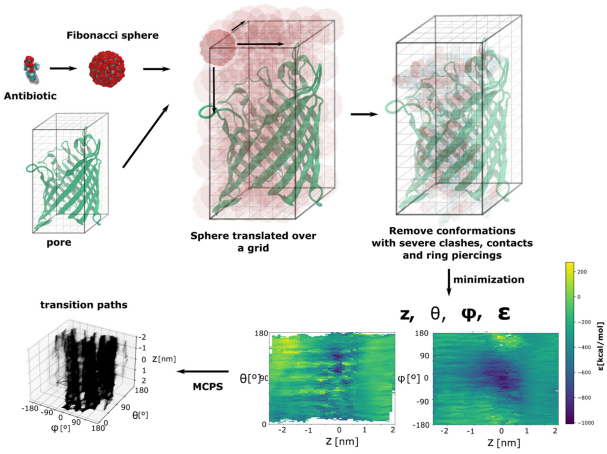

Figure 2: Generation of initial structures for TASS simulation using Monte Carlo Pathway Search (MCPS) *Strategy used for the generation of the MCPS pathways. A Fibonacci sphere of rotational configurations of the antibiotic molecule is translated over a 3D grid covering the pore volume. The data set is cleaned of configurations with clashes, contacts, and ring piercings. The remaining configurations are minimized in the gas phase. For each minimized configuration, the CV z, the inclination angle θ, azimuthal angle , and the protein–antibiotic interaction energy ε are stored. The MCPS algorithm is used to generate the transition paths through the pore. Here, we depict the 5000 trajectories generated for the ENR-OmpK35 system. Reproduces with permission from [8]. Copyright 2025 American Chemical Society.*

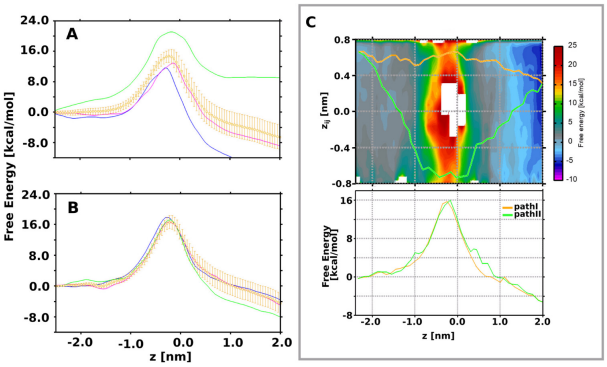

Figure 3: Temperature accelerated sliced sampling (TASS) simulations of Enrofloxacin using with paths generated using SMD and MCPS. A*. Shows the TASS simulation performed using SMD-derived paths.****B****. TASS simulation of MCPS-derived paths.* ***C****. Two-dimensional free-energy estimates for enrofloxacin permeation through the OmpE35 channel obtained from the 3D-Independent MCPS setup. The upper panel shows the free energy within the z vs zij space. The two minimum free-energy paths, path I and path II, were calculated using the zero-temperature string method. The bottom panel depicts the free energy associated with both permeation pathways. Reproduced with the permission from [8]. Copyright 2025 American Chemical Society.*

Our current project focuses on studying more clinically relevant porins, such as *Klebsiella pneumonia*, using the improved MCPS-TASS. Furthermore, we are working on enhancing the electro-osmotic flow (EOF) in porins, as the EOF is the main driving force in transporting neutral solutes. This includes introducing mutations to strengthen the EOF.

WWW

http://www.constructor.university/comp_phys

More Information

[1] J.D. Prajapati et al. *Chem. Rev.*, **121**, 5158-5192 (2021). doi: 10.1021/acs.chemrev.0c01213

[2] S. Acosta-Gutierrez et al. *ACS Infect. Dis.*, **4**, 1487-1498 (2018). doi:10.1021/acsinfecdis.8b00108

[3] E.N. Parker et al. *ACS Cent. Sci.*, **8**, 1145-1158 (2022). doi:10.1021/acscentsci.2c00598

[4] A. Acharya et al. *J. Chem. Theory Comput.*, **17**, 4564–4577 (2021). doi: 10.1021/acs.jctc.1c00369

[5] A. Acharya et al. *J. Chem. Inf. Model.*, **63**, 910–927 (2023). doi:10.1021/acs.jcim.2c01108

[6] A. Acharya et al. *J. Phys. Chem. B*, **127**, 10766–10777 (2023). doi: 10.1021/acs.jpcb.3c04557

[7] A. Acharya et al. *J. Phys. Chem. B*, **128**, 8376–8387 (2024). doi: 10.1021/acs.jpcb.4c03327

[8] A. Acharya et al. *J. Chem. Theory Comput.*, **21**, 3246-3259 (2025). doi: 10.1021/acs.jctc.4c01679

Funding

DFG KL-1299/29-1

DFG Subject Area

201-02 Biophysics